

Vortex phase diagram and quantum fluctuations in thick a - $\text{Mo}_x\text{Si}_{1-x}$ films

S. Okuma, M. Morita, and Y. Imamoto

Research Center for Low Temperature Physics, Tokyo Institute of Technology, 2-12-1, Ohokayama, Meguro-ku, Tokyo 152-8551, Japan

(Received 14 August 2001; revised manuscript received 16 May 2002; published 9 September 2002)

We present measurements of dc and ac complex resistivities for thick amorphous (a -) $\text{Mo}_x\text{Si}_{1-x}$ films. Both the resistivities and the derived vortex-glass-transition line $B_g(T)$ exhibit the decreased temperature T dependence below about 0.1 K. We have proved experimentally that this feature is intrinsic, not resulting from the simple heating effects. We have interpreted this as a sign of a crossover from temperature dominated to quantum driven fluctuations. In the limit $T \rightarrow 0$, the $B_g(T)$ line is T independent and extrapolates to a field $B_g(0)$ lower than the upper critical field $B_{c2}(0)$ at $T=0$, indicative of the presence of the quantum-vortex-liquid phase in the region $B_g(0) < B < B_{c2}(0)$. We show that the $T=0$ phase diagram for the thick films is markedly different from that for the thin films, which is mainly attributed to the different strength of quantum fluctuations between three dimensions and two dimensions. Also, we discuss the difference between the shape of the “melting line” at low T observed in thick amorphous films and single-crystal layered superconductors.

DOI: 10.1103/PhysRevB.66.104506

PACS number(s): 74.25.Dw, 74.40.+k, 74.60.Ec

I. INTRODUCTION

The vortex states and vortex phase diagram of the mixed superconducting state have been actively studied for more than a decade. Although various phases and phase transitions associated with vortex matter have been revealed in the high-temperature regime of the field-temperature (B - T) plane, the vortex states at low T have not yet been fully clarified. This is because most studies performed so far have employed high- T_c oxide superconductors (HTSC's) whose upper critical field B_{c2} at $T=0$ is extremely high.

Quite recently, we have found on the basis of the ac complex resistivity, as well as dc resistivity, for a thick amorphous (a -) $\text{Mo}_x\text{Si}_{1-x}$ film that the vortex-glass transition¹⁻³ (VGT) persists down to $T \sim 0.04T_{c0}$ up to $B \sim 0.9B_{c2}(0)$, where T_{c0} and $B_{c2}(0)$ are the mean-field transition temperature and upper critical field at $T=0$, respectively.⁴ In the limit $T \rightarrow 0$, the VGT line $B_g(T)$ extrapolates to a field below $B_{c2}(0)$, indicative of the presence of a quantum vortex liquid (QVL) at $T=0$ in the regime $B_g(0) < B < B_{c2}(0)$. In fields below $B_g(0)$ the linear (ohmic) dc resistivity $\rho(T)$ exhibits a superconducting transition at nonzero temperatures. The zero-resistivity temperature almost coincides with the VGT temperature $T_g(B)$ determined from the ac resistivity. In fields just above $B_g(0)$, however, $\rho(T)$ decreases from the normal-state resistivity ρ_n upon cooling but tends to the finite nonzero value at $T \rightarrow 0$, suggestive of the ($T=0$) metallic QVL state. We note that all of the data indicate a decreased temperature dependence of the resistivities below about 0.1 K. We interpret this as a sign of a crossover from temperature dominated to quantum driven fluctuations. One may argue, however, that insufficient cooling of the electron system could simply explain the data, because measurements have been performed at very low temperatures ($T < 0.1$ K). It is important to reject such a possibility on the basis of experimental data.

In this paper we first present experimental evidence that the local-heating effects in the sample cannot account for our data. We show that the flattening of $\rho(T)$ observed just

above $B_g(0)$ is intrinsic for our thick [three-dimensional (3D)] films, lending further support for the QVL phase. On the basis of detailed measurements of ac resistivity around $B_g(0)$, we determine the shape of $B_g(T)$ at low T very precisely. The results show that the VGT line $B_g(T)$ is independent of T below about 0.1 K. We also note that the $T=0$ phase diagram (along the field axis) for the thick films is contrasted with that for thin films, which is mainly attributed to the different strength of quantum fluctuations between three and two dimensions. Finally, we point out that the shape of $B_g(T)$ at low T for the thick film is markedly different from that of the “melting line” at low T reported for single-crystal layered oxide⁵ and organic⁶ superconductors. The possible origin of this difference will be discussed. Preliminary results and the transport data related to the present work have been reported elsewhere.^{4,7-10}

II. EXPERIMENT

All of the a - $\text{Mo}_x\text{Si}_{1-x}$ films were prepared by coevaporation of pure Mo and Si in vacuum better than 10^{-8} Torr.^{4,7-13} The films for which we present data in this paper are a 100-nm-thick film ($x=44$ at.%) with $T_{c0}=2.4$ K and $B_{c2}(0)=5.75$ T and a 300-nm-thick film ($x=54$ at.%) with $T_{c0}=3.3$ K and $B_{c2}(0)=7.9$ T. The data of a 4-nm-thick film are also presented for comparison. The structure of the film was confirmed to be amorphous by means of transmission-electron microscopy. Details of the preparation and characterization of the films were published previously.^{8,9,12} The temperature dependence of the linear (ohmic) dc resistivity ρ was measured in constant fields B using standard four-terminal dc and low-frequency (19 Hz) ac locking methods. The field was applied perpendicular to the plane of the film.

The ac transport data, the frequency dependence of the amplitude ρ_{ac} and phase ϕ of the ac resistivity, were also taken in the linear regime as a function of the temperature T and frequency f employing a four-terminal method.^{4,10,14} An oscillator output of the precision LCR meter (HP4285A) produced the current, which passed uniformly through the

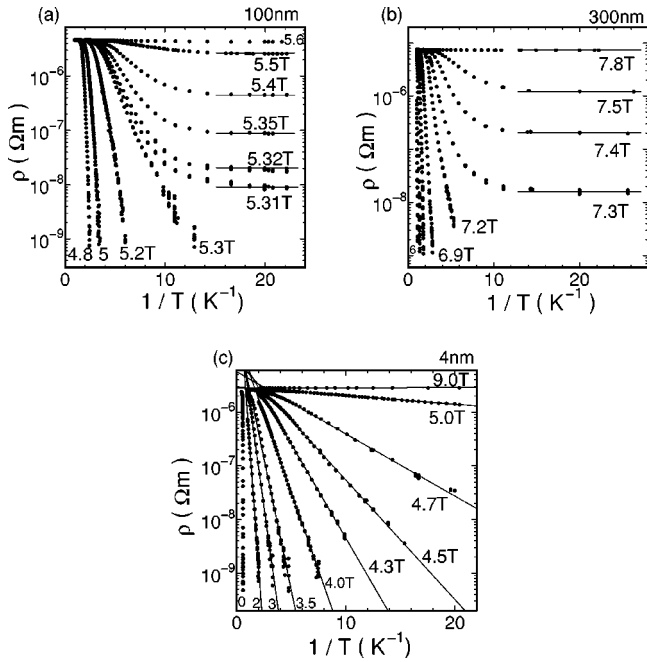


FIG. 1. Arrhenius plots of $\rho(T)$ in different B for the (a) 100-nm-thick, (b) 300-nm-thick, and (c) 4-nm-thick films. For the thicker films the ($T=0$) SMT occurs at around (a) $B=5.3$ and (b) 7.25 T, while for the thin film the ($T=0$) metallic phase is not evident, and is most likely absent.

entire thickness of the film. The ac voltages induced across the sample were measured using the LCR meter after being enhanced with a low-noise preamplifier (NFC SA-430-F5). We regarded the data at the lowest temperature and field as the background data, where ρ_{ac} of the film is much smaller than the background component, and subtracted it from the measured data. We also evaluated a frequency-dependent gain and/or phase delay of the amplifier by measuring the standard noninductive load resistor which was connected in place of the sample. Thus we obtained the frequency-dependent resistivity in the frequency range $f \sim 75$ kHz–5 MHz from the measured voltages. We cannot measure the ac resistivity at lower f (< 75 kHz) because of limitation of the LCR meter. However, the essential data is included in the f range used in the present measurement. This has been verified by the simultaneous measurements of dc (current density J vs resistivity ρ) and ac complex resistivities (ρ_{ac} and ϕ) for the thick film in low B (≤ 1 T), where convincing evidence for VGT has been obtained from both measurements consistently.¹⁰ Even if we tried to perform the measurement at lower f (< 75 kHz), ρ_{ac} around T_g would fall below the experimental resolution of our preamplifier.¹⁵

III. RESULTS AND DISCUSSION

Figures 1(a)–1(c) show the Arrhenius plots of the dc resistivity $\rho(T)$ in different B for the 100-nm-thick, 300-nm-thick, and 4-nm-thick films, respectively. The data for the 4-nm-thick film ($x = 61$ at. %) with $T_{c0} = 1.8$ K shown in Fig. 1(c) were taken simultaneously with those of the 100-nm-

thick film shown in Fig. 1(a) in our ^3He - ^4He dilution refrigerator. For the thicker (100- and 300-nm) films we can roughly confirm that $\rho(T)$ follows the power-law functional form predicted by the vortex-glass (VG) theory in fields below the certain characteristic field B_0 , where $B_0 \approx 5.3$ and 7.2 T for the 100-nm-thick and 300-nm-thick films, respectively. In fields B higher than B_0 ($5.31\text{ T} \leq B \leq 5.6$ T and $7.3\text{ T} \leq B \leq 7.8$ T for the 100-nm-thick and 300-nm-thick films, respectively), however, the logarithm of $\rho(T)$ decreases with upward curvature below about 0.1 K and the finite temperature independent ρ (the so-called “flat tail”) remains at lowest temperatures.⁴ The temperature range is not broad enough to definitely claim the $T=0$ metallic phase, while we do not observe any sign of insulating behavior, such as a minimum of ρ and a subsequent increase in ρ at $T \rightarrow 0$, as reported in other thin-film superconductors,¹⁶ down to the lowest T measured.

From an experimental point of view, one may argue that the flattening of $\rho(T)$ at low T is not intrinsic but merely resulting from local-heating effects of the electron system. That is, the temperature of the samples could not follow the thermometer but deviated below about 0.1 K and remained at higher temperature. This question, which is frequently asked but difficult to answer definitely, is important in interpreting the data at very low T (< 0.1 K) properly. Empirically, the following facts may rule out the possibility: The power dissipated in our film is typically about 1 pW in the normal state and about 10 fW at the lowest temperatures and fields where the flattening of $\rho(T)$ was observed. These values are sufficiently lower than the values of the power generated in the usual transport measurements in the 40-mK range. Furthermore, the cooling power of our dilution refrigerator is 100 μW at 100 mK, which is much larger than the power dissipated in the sample including lead wires and contacts.

In the discussion which follows, we will show more evidence that heating effects do not seriously affect our data. It is seen from Fig. 1(c) that for the 4-nm-thick film the resistance in $B < B_{SI}^{2D}$ follows an Arrhenius-type temperature dependence down to the lowest T (≈ 0.05 K) without showing the flat tail, where B_{SI}^{2D} is the critical field of the 2D field-driven superconductor-insulator transition (SIT) at $T=0$. Such behavior would not be expected if there were large deviations between the temperatures of the sample and thermometer. Accordingly, it is reasonable to consider that the flattening of $\rho(T)$ at $T \rightarrow 0$ observed for thicker films is intrinsic. If we assume that the flat tail persists down to $T=0$, $B_0 \approx 5.3$ and 7.25 T are identified with the critical fields B_{SM}^{3D} of the (3D) superconductor-metal transition (SMT) at $T=0$ for 100-nm-thick and 300-nm-thick films, respectively. It is also important to note that the slope (activation energy) extracted from the plot in Fig. 1(c) exhibits the $\log B$ dependence predicted by the 2D dislocation model.¹⁷ This is consistent with a view that the transport (ρ) in the presence of perpendicular fields is indeed dominated by flux motion. This view, which has been usually believed without experimental proof, will be further supported by the observation of VGT on the basis of ac resistivity for the thick film, as described below.

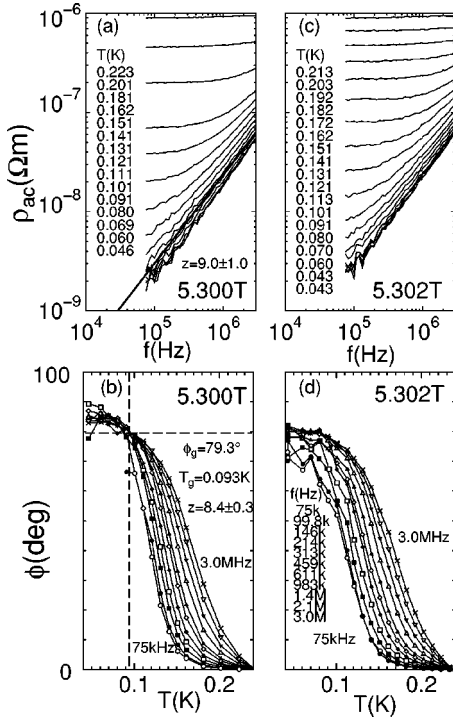


FIG. 2. (a) Frequency dependence of the amplitude $\rho_{ac}(f)$ and (b) temperature dependence of the phase $\phi(T)$ of the linear ac resistivity for the 100-nm-thick film in a constant field $B = 5.300$ T. A straight line in (a) represents T_g . (c) ρ_{ac} vs f and (d) ϕ vs T in $B = 5.302$ T. For (a) and (c) temperatures of the isotherms are listed in the figures (from the top to the bottom). For (b) the frequencies follow the same sequence as those listed in (d) (from the left to the right).

Figures 2(a) and 2(b), respectively, show the frequency dependence of the amplitude ρ_{ac} and temperature dependence of the phase ϕ of the linear ac resistivity for the 100-nm-thick film in a constant field $B = 5.300$ T. Upon cooling from about 0.35 K, ρ_{ac} shows a steep decrease, while both ρ_{ac} and ϕ exhibit an increase at high f . With further decreasing T , the increase in ρ_{ac} and ϕ at high f becomes more remarkable and the characteristic frequency above which they start to increase shifts to the lower f . This behavior is characteristic of the critical slowing down of the vortex dynamics near the second-order transition.² We find that ϕ at different f merges to the same value $\phi_g \approx 79.3^\circ$ at $T \approx 0.093$ K, indicating that the VGT occurs at $T_g \approx 0.093$ K.¹⁸ Using $\phi_g = 79.3^\circ$, the dynamical exponent z is immediately obtained to be 8.4 ± 0.3 from the relation $\phi_g = (\pi/2)(z-1)/z$. At T_g , ρ_{ac} exhibits a power-law frequency dependence, $\rho_{ac} \propto f^{(z-1)/z}$, predicted by the VGT theory, as shown with a straight line in Fig. 2(a), yielding $z = 9.0 \pm 1.0$. The behavior presented here is essentially similar to that which has been observed for lower fields ($1.0 \leq B < 5.2$ T) except that z in $B = 5.1$ – 5.3 T takes somewhat higher values 8.1 – 8.5 than those ($z \sim 6$) in lower fields $B = 1.0$ – 5.0 T.⁴

We now comment on the measurements of (dc) J - ρ characteristics, because the J - ρ measurements are more com-

monly used to claim the VGT (Refs. 19–23) than are ac measurements.^{14,24–26} As mentioned above, we have already reported the results of the simultaneous measurements of dc and ac complex resistivities in low B (≤ 1 T) at high T (> 1 K) and proved the existence of VGT consistently.¹⁰ However, in the low- T and high- B regime that we focus on in the present study, it is difficult to determine T_g as well as z precisely based on the dc data alone. This is because at lower T heating effects become more unignorable in J - ρ measurements. In order to determine the shape of J - ρ characteristics to be compared with the VG theory, we must perform measurements up to the relatively high- J region. Furthermore, at lower T , J - ρ curves shift to higher J and hence, heating effects, which may affect the shape of the J - ρ curves, become more serious. We emphasize that ac measurements are advantageous over dc ones at low temperature since joule heating produced in the sample can be small compared with that in the dc measurements. We believe that the ac complex resistivity measurement performed in this study is the only reliable method to demonstrate the VGT at very low temperatures.

Let us turn to the results of ac resistivity at higher fields. The breakdown of the critical behavior of VGT is noticeable in $B \geq 5.31$ T, where ρ_{ac} does not obey the power-law frequency dependence down to the lowest T and ϕ does not merge at any angle lower than 90° . In order to see how the critical behavior breaks down with increasing B more closely, we have measured ρ_{ac} and ϕ in a field of $B = 5.302$ T, which is only slightly higher than 5.300 T, as shown in Figs. 2(c) and 2(d), respectively. Experimentally, we are not able to guarantee the absolute value of $B = 5.300$ or 5.302 T, because we do not measure the strength of the magnetic field directly with the precision of 1 mT. However, the difference between $B = 5.302$ T and $B = 5.300$ T is precisely estimated from the current of the magnet. Seemingly, the power-law frequency dependence of ρ_{ac} is also observed in 5.302 T at lowest temperatures; however, the crossing behavior of ϕ is no longer visible. Only an addition of $\Delta B = 2$ mT, which corresponds to $\Delta B/B \approx 0.04\%$, drastically causes destruction of VGT.

The implication of this result is that the VGT line $B_g(T)$ runs parallel with the T axis below about 0.1 K, extrapolating to a field between 5.300 and 5.302 T in the limit $T \rightarrow 0$. One can also see from these results that the phase ϕ is much more sensitive than the amplitude ρ_{ac} in judging the existence of VGT.⁴ Since the fields 5.302 and 5.300 T are very close to each other, the temperature region of $\phi(T, f)$ shown in Fig. 2(d) is also nearly identical to that shown in Fig. 2(b). Accordingly, the abrupt change in $\phi(T, f)$ observed between $B = 5.300$ and 5.302 T cannot be explained in terms of simple heating effects but should be attributed intrinsically to field effects. This finding further contradicts the argument that the decreased temperature dependence of $B_g(T)$, as well as that of dc $\rho(T)$, below about 0.1 K might be due merely to insufficient cooling of the electron system. We thus claim that 5.3 T is indeed the upper bound $B_g(0)$ of the VG phase. Coincidence of this boundary field $B_g(0)$ determined from ac resistivity with B_{SM}^{3D} determined from dc resistivity [Fig.

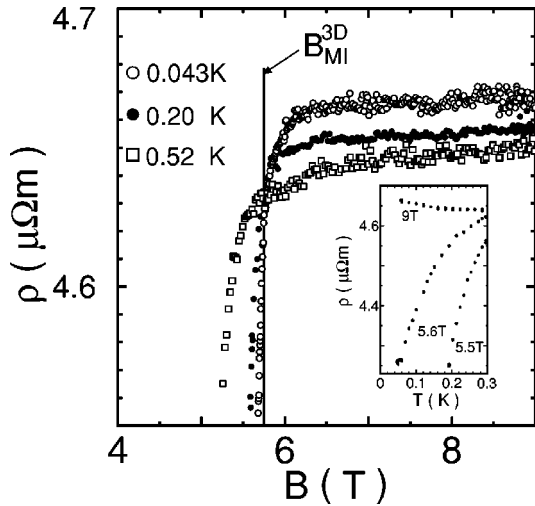


FIG. 3. Field dependence of $\rho(B)$ for the 100-nm-thick film at different T . The ($T=0$) critical field B_{MI}^{3D} of MIT is estimated to be 5.75 T from an intersection point. Inset: Temperature dependence of ρ in different B .

1(a)] indicates that both ac and dc measurements detect an intrinsic phenomenon (phase transition) which occurs at $B = 5.3$ T below 0.1 K.

In order to discuss the (B - T) phase diagram for the thick (100-nm) film, we estimate the critical field B_{MI}^{3D} of the metal-insulator transition (MIT) at $T=0$ as well as the upper critical field B_{c2} , where B_{c2} is defined as a field above which all evidence for the electron pairs disappears. As shown in the inset of Fig. 3, upon cooling, the dc resistivity $\rho(T)$ in $B \leq 5.6$ T exhibits a decrease, while $\rho(T)$ in $B = 9$ T shows a slight increase, indicative of insulating behavior. In the main panel of Fig. 3 the field dependence of $\rho(B)$ at different T is plotted. From an intersection point of the isotherms at low T ,²⁷ the ($T=0$) critical field B_{MI}^{3D} of MIT is estimated to be about 5.75 T. In B higher than about 6 T, which is close to B_{MI}^{3D} , $\rho(B)$ at low T is almost constant or shows a slight increase with increasing B , suggesting that the origin of the magnetoresistivity (MR) in this field region is due to unpaired electrons. Thus, the upper critical field $B_{c2}(0)$ is considered to be close to (or slightly higher than) $B_{MI}^{3D} = 5.75$ T. This is in contrast to the result for thin films, in which an anomalous peak and a subsequent decrease in the MR suggesting the existence of localized electron pairs have been observed over the broad field region $B_{SI}^{2D} < B < B_{c2}(0)$.⁸

The temperature variation of the upper critical field $B_{c2}(T)$ is obtained from the resistive transition. In a previous report⁴ we have used a criterion that $\rho(T)$ decreases to 90% of the normal-state resistivity ρ_n to determine $B_{c2}(T) [\equiv B^{0.90}(T)]$ and showed that $B_{c2}(T)$ thus obtained is extrapolated to about 5.7 T in the limit $T \rightarrow 0$, consistent with the estimation of $B_{c2}(0)$ mentioned above. Since in this paper we have more detailed discussions on the shape of the low- T phase diagram, we should adopt an alternative criterion, such as the 95% [$B^{0.95}(T)$] or 99% [$B^{0.99}(T)$] criterion, which reflects a true $B_{c2}(T)$ better than $B^{0.90}(T)$. In Fig. 4

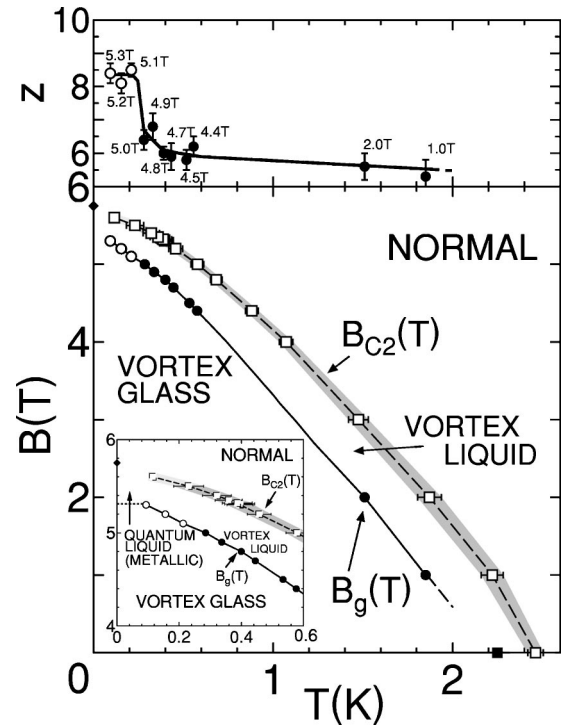


FIG. 4. Top: Dynamical exponents z for the VGT plotted against $T_g(B)$ for the 100-nm-thick film. Open circles represent the points for $B = 5.1$ – 5.3 T where z takes somewhat higher values 8.1–8.5 than those ($z \sim 6$) for lower fields $B = 1.0$ – 5.0 T. Bottom: B - T phase diagram of the 100-nm-thick film over the whole T range. Circles and open squares denote $B_g(T)$ and $B^{0.95}(T)$, respectively. Open circles represent $B_g(T)$ ($= 5.1$ – 5.3 T) where values of z are higher than those for lower fields $B = 1.0$ – 5.0 T. $B_{c2}(T)$ is shown with the shaded zone. A diamond denotes $B_{MI}^{3D} \sim B_{c2}(0)$. A filled square corresponds to the zero-resistivity temperature in $B = 0$. Inset: The low- T part of the phase diagram. A dotted line marks the upper bound of the VG phase. The full and dashed lines are guides for the eyes.

(bottom panel) we plot $B^{0.95}(T)$ (with the open squares) instead of $B^{0.99}(T)$, because it is difficult to determine $B^{0.99}(T)$ from the measured $\rho(T)$ without great ambiguity. Considering that physically, $B_{c2}(T)$ is not a true phase transition, we illustrate the location of $B_{c2}(T)$ with the shaded zone. The left (lower) bound of the zone is identical to $B^{0.90}(T)$, while the right (upper) bound corresponds to a line that is obtained by shifting the $B^{0.95}(T)$ line by $\Delta T(B)$ along the T axis, where $\Delta T(B)$ is the temperature difference between the $B^{0.95}(T)$ and $B^{0.90}(T)$ lines for each B . As clearly seen from the inset of Fig. 4, the right (upper) bound is extrapolated to $B_{c2}(0) \approx 5.75$ T (shown with a diamond) more smoothly than the left (lower) one $B^{0.90}(T)$.

In contrast to $B_{c2}(T)$, the VGT field $B_g(T)$ is well determined. The filled and open circles in Fig. 4 (bottom panel) represent T_g for different B determined from the phase ϕ of the ac resistivity. Open circles denote the particular points for $B = 5.1$, 5.2, and 5.3 T where values of z are higher than those for lower B .⁴ As shown in Fig. 4 (top panel), an abrupt jump in z is clearly visible at $B \approx 5.0$ T and $T = 0.24 \pm 0.04$ K, which correspond to 87% of $B_{c2}(0)$ and 10% of

T_{c0} , respectively. The reason for the jump in z is not clear; however, it may reflect the crossover from the thermal to quantum liquid regime. As described above, in the limit $T \rightarrow 0$, $B_g(T)$ extrapolates to a field between 5.300 and 5.302 T, that is in good agreement with $B_{SM}^{3D} \approx 5.3$ T. This field is apparently lower than $B_{c2}(0)$, indicative of a metallic QVL state in the region $B_g(0) < B < B_{c2}(0)$. However, we cannot tell definitely from the present data whether the VGT actually persists down to $T=0$ in the very narrow field region $5.300 \text{ T} < B < 5.302 \text{ T}$, as shown with a dotted line in the inset of Fig. 4. We notice that, if the VGT actually persists down to $T=0$, the slope of the VGT line $B_g(T)$ seems to exhibit a discontinuous drop at around 0.09 K. It is not evident whether this abrupt change in the slope is intrinsic and, if so, it is physically plausible.

We consider that part of the reason may be due to spatial distribution of $T_g(B)$ originating from the possible inhomogeneity of Mo concentration in the sample, which cannot be detected within our experimental resolutions of sample characterization. We emphasize that our film is highly homogeneous, which is guaranteed by the crossing behavior of the phase ϕ at $T_g(B)$ in different B spanning over the broad range. Nevertheless, in the field region just above 5.300 T where the VGT line $B_g(T)$ is nearly independent of temperature, the presence of a very small inhomogeneity of the sample gives rise to the considerable distribution of $T_g(B)$ ($=0-0.09$ K) within the sample, which in turn results in smearing or disappearance of crossing behavior of ϕ . Thus, the upper bound of the VG phase at $T \rightarrow 0$, $B_g(0)$, shown with the dotted line in the inset of Fig. 4 might be slightly underestimated, leading to the seemingly abrupt change in the slope of $B_g(T)$ at around 0.09 K.

To summarize, we have obtained the precise shape of $B_g(T)$ at low T as well as clear evidence for VGT. We have revealed that the QVL regime is present at $T \rightarrow 0$ in B lower than $B_{c2}(0)$, which is most likely metallic. However, we cannot claim the existence of the $T=0$ metallic phase definitely, because flattening of $\rho(T)$ is observed only in a limited temperature range $0.019 < T/T_{c0} < 0.03$. This problem should be clarified in future experiments, since theoretically the existence of the $T=0$ metallic phase below $B_{c2}(0)$ has not been fully justified.²⁸ To prove or disprove the $T=0$ metallic phase, further measurements down to even with lower T/T_{c0} (< 0.019) are necessary. For this purpose, we must prepare films with higher T_{c0} , since the lowest temperature available in our transport measurements is limited to around 0.04 K. As T_{c0} is higher, however, the film is less disordered (ρ_n is lower) and hence, the strength of quantum fluctuations is expected to be weaker. This will lead to suppression of QVL, making it difficult to observe the ‘‘metallic’’ QVL phase. While further experiments are strongly required, it is not straightforward to demonstrate the $T=0$ metallic state in the QVL phase.

There are several theories²⁹⁻³⁵ which predict quantum melting of the vortex solid; however, most of them have focused on melting of the vortex lattice in clean systems and effects of quantum fluctuations on the VGT have not been fully studied. In the absence of appropriate theories, we have

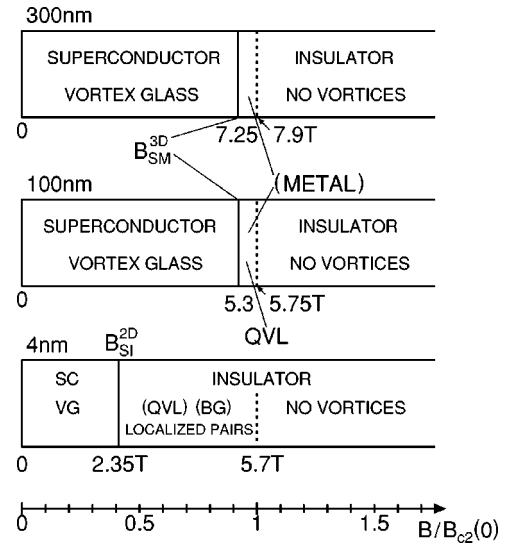


FIG. 5. The $T=0$ phase diagrams along the field axis for the thick (3D) films with thickness of 300 ($\rho_n = 7.8 \mu\Omega \text{ m}$) and 100 nm ($\rho_n = 4.6 \mu\Omega \text{ m}$) and for an ultrathin (2D) film with thickness of 4 nm ($\rho_n = 7.2 \mu\Omega \text{ m}$). The field axis is normalized by $B_{c2}(0)$ for each film. The QVL phase is well defined for the 3D films, while we have not yet obtained convincing evidence for the 3D metal phase just above B_{SM}^{3D} as well as 2D QVL [Bose-glass (BG)] phase. Note that the Meissner phase, which corresponds to $B=0$, is not shown here.

heuristically analyzed our data using the melting theory of the vortex lattice which takes account of quantum fluctuations. We make use of a theory by Blatter and co-authors^{29,30} which has been constructed based on a Lindemann-like criterion. We note, however, that theoretically the Lindemann-like approach is considered to be a rough thermodynamic estimation.²⁸ We use the theory, because the numerical evaluation given in the theory can be easily compared with the experimental data. In fact, it has been widely used to analyze the data in various type-II superconductors.^{5,6,30,36,37}

According to the theory, the width of the QVL phase at $T=0$, $B_{c2}(0) - B_m^q(0)$, is determined by the strength of quantum fluctuations, which is quantified by the resistance ratio $\rho_n/R_q d$. Here, $R_q = h/2\pi e^2 \approx 4.1 \text{ k}\Omega$ is the quantum resistance and d is the relevant scale for the fluctuations, the interlayer spacing for HTSC's and the superconducting coherence length or film thickness for uniform films. The relative width of the ($T=0$) QVL phase normalized by $B_{c2}(0)$ is expressed as

$$\begin{aligned}
 \Delta B_{QVL} &= [B_{c2}(0) - B_m^q(0)]/B_{c2}(0) \\
 &= \frac{2}{\pi} \exp\left(\frac{2\pi}{3} \alpha - \frac{\alpha^2}{2} - \frac{\pi^3 c_L^2}{2} \frac{R_q}{R_n^*}\right), \quad (1)
 \end{aligned}$$

where c_L is the Lindemann number, $\alpha = 2/\sqrt{\pi} \nu$ (ν is a numerical constant of order unity), and $R_n^* = \rho_n \nu / a_0$ ($a_0^2 = \Phi_0/B$ is the unit-cell area and Φ_0 the flux quantum). Identifying $B_m^q(0)$ with $B_g(0)$, we obtain nearly common values of $\Delta B_{QVL} \approx 0.07-0.08$ from the measured values of $B_{c2}(0)$

and $B_g(0)$ (or B_{SM}^{3D}) both for 100-nm-thick and 300-nm-thick films (see also the phase diagram in Fig. 5). Taking $\nu=1$ and inserting $\Delta B_{QVL}=0.075$ and $\rho_n=4.6 \mu\Omega \text{ m}$ into Eq. (1), the Lindemann number c_L for the 100-nm-thick film is calculated to be 0.12, which is of reasonable magnitude.^{4,30} For the 300-nm-thick film with $\rho_n=7.8 \mu\Omega \text{ m}$, the strength of quantum fluctuations quantified by $\rho_n/R_q d$ ($d=a_0$) is about twice as large as that for the 100-nm-thick film. If we again use $c_L=0.12$ and $\nu=1$, ΔB_{QVL} for the 300-nm-thick film is calculated to be about 0.5, which is much larger than the measured value of 0.08. This result means that we cannot use a common value of $c_L(=0.12)$ and $\nu(=1)$ for films with different thicknesses prepared independently³⁸ or that the width of the QVL phase is not determined only by the magnitude of $\rho_n/R_q d$. The latter explanation is not unreasonable, considering that ΔB_{QVL} depends not only on the magnitude of quantum fluctuations but also on the strength of flux pinning that is determined by the microscopic or mesoscopic morphology of the film. The narrower QVL phase for the 300-nm-thick film than has been predicted [Eq. (1)] may be attributed to enhanced pinning effects for the thicker film. Taking this fact into consideration, we are now conducting experiments using a series of $a\text{-Mo}_x\text{Si}_{1-x}$ films with varying x (ρ_n) but fixed film thickness. These films are prepared simultaneously and hence, except for the difference in Mo concentration x , the microscopic or mesoscopic morphology of the films responsible for pinning is expected to be similar to each other. Thus we are able to elucidate the effects of disorder (ρ_n) or quantum fluctuations on the phase diagram. The same sample-preparation method has been employed in fabricating 4-nm-thick films for the study of the 2D SIT.^{8,9,12}

Shown in Fig. 5 are the $T=0$ phase diagrams along the field axis for thick (3D) films with thickness of 300 and 100 nm and the (possible) phase diagram for an ultrathin (2D) film with thickness of 4 nm. For comparison, the field axis is normalized by $B_{c2}(0)$ for each film. It can be seen that the phase diagrams for the thick films are similar to each other: In fields lower than B_{SM}^{3D} , there is the superconducting VG phase. Above B_{SM}^{3D} , there is the QVL regime, which is most likely metallic. This goes to the normal phase (Fermi insulator) at $B_{c2}(0)$ ($\sim B_{MI}^{3D}$), where neither electron pairs nor vortices are present. The QVL phase ΔB_{QVL} is well defined, though it is narrow; $\Delta B_{QVL} \sim 0.07\text{--}0.08$.

The phase diagram for the thin (2D) films is contrasted with that for the thick (3D) films. Typically shown in Fig. 5 is the result for the 4-nm-thick film with $\rho_n=7.2 \mu\Omega \text{ m}$, which is close to $\rho_n=7.8 \mu\Omega \text{ m}$ for the 300-nm-thick film. The transport data of the 4-nm-thick film, which are used to construct the phase diagram, have been presented elsewhere.⁸ In the case of 2D, there is a well-defined critical field B_{SI}^{2D} of the SIT separating the insulating phase from the superconducting (VG) phase. The metallic QVL phase below B_{SI}^{2D} , which has been reported in different thin-film (2D) superconductors,^{16,36,37} is not evident, and is most likely absent.⁸ Instead, there is the broad unusual insulating regime [$B_{SI}^{2D} < B < B_{c2}(0)$] suggesting the presence of the localized electron pairs,⁹ as described above. According to the theory of Fisher,³⁹ this regime is interpreted as the *insulating* QVL

phase, the so-called Bose-glass (BG) phase, originating from strong quantum fluctuations in two dimensions. This goes to the Fermi insulator at $B_{c2}(0)$, which is close to the critical field $B_{\parallel C}$ ($= 5.7 \text{ T}$) for the parallel orientation (the field applied parallel to the film surface).⁸ From the systematic studies on a series of thin films with different disorder (ρ_n), we have found that the relative width of the unusual insulating (or the QVL) regime, defined by $\Delta B_{(QVL)} = [B_{c2}(0) - B_{SI}^{2D}] / B_{c2}(0)$, grows as disorder of the film increases.⁸ The value of $\Delta B_{(QVL)}$ for the thin (4-nm) film whose disorder (ρ_n) is close to that for the present 100-nm-thick film is about 0.25,⁸ which is still larger than the width of the metallic QVL regime ($\Delta B_{QVL} \sim 0.075$) for the thick film. This result is mainly attributed to the stronger quantum-fluctuation effects for thinner (2D) films.

Here, we comment on the dimensionality of the vortex system. The existence of 3D VGT in disordered films with thickness of order 100 nm has been demonstrated⁴⁰ both in low- T_c (Refs. 4, 10, 22, and 26) and high- T_c (Refs. 19–21) films. In our previous work, as well as the present paper, we have studied disordered superconducting films, such as In (Refs. 22 and 26) and $a\text{-Mo}_x\text{Si}_{1-x}$ (Refs. 4 and 10) films, which exhibit the VGT. Therefore, the dimensionality discussed in our papers is specifically that for the VGT, which is different from that discussed for less disordered superconductors.^{41–43} For $a\text{-NbGe}$ (Ref. 41) and $a\text{-MoGe}$ (Ref. 42) films having nearly the same thickness as our thick $a\text{-Mo}_x\text{Si}_{1-x}$ films the ac and dc data show the behavior in favor of 2D melting of the vortex lattice. In particular, a sudden drop in the imaginary part of the ac conductance G , together with a distinct peak in the real part of G , reported in Ref. 42, impressively signals the 2D melting transition. This is in contrast to the result for our thick films.

We consider that this difference is attributed to a stronger pinning effect in our $a\text{-Mo}_x\text{Si}_{1-x}$ films than in $a\text{-NbGe}$ and $a\text{-MoGe}$ films: The strength of pinning in our films is high enough for the 3D VGT (rather than 2D melting transition) to be visible. The following facts may support this notion: (i) Reported values of ρ_n for $a\text{-NbGe}$ (Ref. 41) and $a\text{-MoGe}$ (Ref. 42) films are 1.5 and 2 $\mu\Omega \text{ m}$, respectively, which are certainly lower than 5 and 8 $\mu\Omega \text{ m}$ for our $a\text{-Mo}_x\text{Si}_{1-x}$ films. (ii) We have previously performed measurements of current-driven voltage noise S_V as a function of B .¹³ The results show that a *broad* peak in $S_V(B)$ originating from plastic-flow motion of the vortex solid (VG) is observed below B_g . This is in contrast to the results for less disordered superconductors⁴⁴ where noise is localized in a *narrow* range of B just prior to melting of the vortex lattice B_m . (iii) In ultrathin (3-nm) films of $a\text{-MoGe}$ the flattening of the resistance, which has been interpreted in terms of quantum tunneling of vortices, is observed at low T in fields well below B_{MI} .¹⁶ As mentioned above, the behavior is different from that for our ultrathin (4-nm) films of $a\text{-Mo}_x\text{Si}_{1-x}$. This difference may again reflect the fact that pinning in our $a\text{-Mo}_x\text{Si}_{1-x}$ films is more effective than in $a\text{-MoGe}$ films. It is also noted that evidence for the VGT has been detected in a clean untwinned single crystal of $\text{YB}_2\text{Cu}_3\text{O}_{7-\delta}$ with in-

duced pointlike disorder, in which the first-order melting transition has been completely suppressed after proton irradiation.⁴⁵

Finally, we discuss the shape of the melting line $B_m(T)$ [or the irreversibility line $B_{irr}(T)$] at low T obtained in different type-II superconductors.^{5,6} In the overdoped single crystal $\text{Bi}_{2+x}\text{Sr}_{2-(x+y)}\text{Cu}_{1+y}\text{O}_{6\pm\delta}$ with $T_{c0}\approx 4$ K,⁵ the irreversible field $B_{irr}(T)$ has been reported to exhibit an upward curvature, which is in good agreement with the form predicted by the Lindemann criterion for the melting of a three-dimensional (3D) anisotropic vortex lattice.⁴⁶ The upward curvature $B_{irr}(T)$ reproduced by the Lindemann form persists down to low enough T (~ 60 mK), whereas alternative models based on quantum melting,²⁹ 2D melting,⁴⁷ and flux creep⁴⁸ have been shown to be unsuitable to describe the data. What is noted in the report is the absence of quantum-fluctuation effects even at very low temperatures $T/T_{c0}=0.015$. This is in contrast to the result for the anisotropic layered organic superconductor $\kappa\text{-(BEDT-TTF)}_2\text{Cu(NCS)}_2$ with $T_{c0}\sim 9$ K,⁶ where BEDT-TTF denotes bis(ethylenedithio)tetrathiafulvalene. In this system the existence of a QVL state has been claimed on the basis of the finding of the finite field region $B_{irr}\leq B\leq B_{c2}$ at $T=0$. It should be mentioned that in these single-crystal layered superconductors the type of the melting transition (i.e., whether the transition is first order or second order), as well as the exact shape of the melting line, has not been well determined. As the authors in Refs. 5 and 6 have correctly admitted themselves, this is because what they have measured is the irreversible field B_{irr} instead of the melting field B_m . Nevertheless, it is not unreasonable for the authors to expect that B_m lies close to B_{irr} and hence, the arguments on the finite QVL state at $T=0$ in Ref. 6 seem to be valid.

Hereafter, assuming that $B_{irr}\approx B_m$, we compare the low- T phase diagrams for layered superconductors with those for amorphous films. The most remarkable feature is that in the layered single-crystal superconductors^{5,6} the derivative of $B_{irr}(T)$, dB_{irr}/dT , in the limit $T\rightarrow 0$ approaches $-\infty$ [i.e., an increasing upward curvature of $B_{irr}(T)$ persists down to lowest temperatures measured] or takes appreciable negative values, while in our amorphous film $dB_g/dT\approx 0$ at $T\rightarrow 0$. The T -independent portion of B_m has been also reported in thick amorphous Nb_3Ge films with *less* disorder, where the first-order transition is observed.³⁶

The theory for clean superconductors^{30,31,33} has predicted the T independent $B_m(T)$ driven by quantum fluctuations at low enough T , which cannot account for the results of layered superconductors. According to the VG theory of Fisher *et al.*,^{2,39} on the other hand, the vortex phase diagram at low T is largely dependent on dimensionality of the system. When the dimensionality is lower than three, the $B_g(T)$ line for three dimensions is suppressed and instead the vortex-liquid phase below $B_{c2}(T)$ is enhanced. For ideally 2D superconductors with moderately strong disorder, the phase transition from the VG to QVL (BG) phase occurs at $T=0$ (Fig. 5), while only the vortex-liquid phase is present in

fields below $B_{c2}(T)$ at nonzero temperatures $0<T<T_{c0}$.^{39,49} We suggest that the finite nonzero slope of $B_{irr}(T)$ at $T\rightarrow 0$ reported in different quasi-2D layered superconductors may imply, in contrast to the general belief, that these systems essentially undergo the second-order transition at least at low T . Within this interpretation, in the limit of large anisotropy, the slope of $B_{irr}(T)$ at $T=0$ tends to $-\infty$ and the system approaches the one described by the 2D VGT picture.³⁹ We propose that ac complex resistivity (susceptibility) measurements should be performed for these single-crystal layered superconductors to test this interpretation. It may be also intriguing to investigate the amorphous superconductor/insulator multilayer films in which anisotropy of the system can be readily controlled.^{50,51} Using $a\text{-W/Si}$ multilayer films,⁵¹ for example, roles of anisotropy on the VGT at low T may be systematically studied. As an extension of present work, we are studying quasi-2D $a\text{-Mo}_x\text{Si}_{1-x}$ films with thickness between 4 and 100 nm to clarify the effects of reduced dimensionality on the phase diagram.

In summary, we have presented measurements of dc and ac complex resistivities for thick $a\text{-Mo}_x\text{Si}_{1-x}$ films. (i) Both the resistivities and the VGT line $B_g(T)$ exhibit the decreased temperature dependence below about 0.1 K ($T/T_{c0}<0.04$). We have proved experimentally that this feature is intrinsic, not resulting from the simple heating effects. We have interpreted this fact, together with the finding of an abrupt increase in the dynamical exponent z below about 0.24 K ($T/T_{c0}<0.1$), as a sign of a crossover from temperature dominated to quantum driven fluctuations. (ii) On the basis of detailed measurements around $B_g(0)$, the precise shape of $B_g(T)$ at low T has been determined. In the limit $T\rightarrow 0$, the $B_g(T)$ line is independent of T and extrapolates to a field $B_g(0)$ lower than $B_{c2}(0)$, lending strong support for the QVL phase in the field region $B_g(0)<B<B_{c2}(0)$. (iii) We have compared the $T=0$ phase diagram for the thick films with that for the thin films. The anomalous insulating regime suggestive of QVL is commonly observed for thin films. This regime is much wider than the “metallic” QVL regime for thicker films. This is mainly attributed to the enhanced quantum-fluctuation effects in two dimensions. (iv) Finally, we have argued that for the single-crystal layered superconductors the slope of $B_{irr}(T)$ at $T\rightarrow 0$ takes appreciably negative values, which is in contrast to the results for amorphous films. We suggest that the VGT may also occur at low T in the single-crystal layered superconductors. Within this interpretation, the difference in the low- T “melting” line between these two systems is attributed to different dimensionality.

ACKNOWLEDGMENTS

We thank R. Ikeda and T. Onogi for useful discussions. This work was supported by a Grant-in-Aid for Scientific Research (B) from the Ministry of Education, Science, Sports, and Culture.

- ¹M. P. A. Fisher, Phys. Rev. Lett. **62**, 1415 (1989).
- ²D. S. Fisher, M. P. A. Fisher, and D. A. Huse, Phys. Rev. B **43**, 130 (1991).
- ³A. T. Dorsey, Phys. Rev. B **43**, 7575 (1991).
- ⁴S. Okuma, Y. Imamoto, and M. Morita, Phys. Rev. Lett. **86**, 3136 (2001); in *Proceedings of the Third International Conference on New Theories, Discoveries and Applications of Superconductors and Related Materials, Honolulu, 2001*, edited by J. D. Fan [Physica C **364-365**, 526 (2001)].
- ⁵A. Morello, A. G. M. Jansen, R. S. Gonnelli, and S. I. Vedenev, Phys. Rev. B **61**, 9113 (2000).
- ⁶T. Sasaki, W. Biberacher, K. Neumaier, W. Hehn, K. Andres, and T. Fukase, Phys. Rev. B **57**, 10 889 (1998).
- ⁷S. Okuma, Y. Imamoto, and M. Morita, in *Proceedings of the 13th International Symposium on Superconductivity, 2000, Tokyo*, edited by K. Kitazawa and Y. Shiohara, Physica C **357-360**, 466 (2001).
- ⁸S. Okuma, S. Shinozaki, and M. Morita, Phys. Rev. B **63**, 054523 (2001); S. Okuma and M. Morita, in *Proceedings of the 13th International Symposium on Superconductivity, 2000, Tokyo*, edited by K. Kitazawa and Y. Shiohara, Physica C **357-360**, 556 (2001).
- ⁹S. Okuma, T. Terashima, and N. Kokubo, Phys. Rev. B **58**, 2816 (1998).
- ¹⁰S. Okuma and M. Arai, J. Phys. Soc. Jpn. **69**, 2747 (2000).
- ¹¹It has been shown previously that an amorphous-film system, such as $a\text{-Si}_{1-x}\text{Au}_x$, is suitable for the study of the electron localization and superconductor-insulator transition [N. Nishida, T. Furubayashi, M. Yamaguchi, K. Morigaki, and H. Ishimoto, Solid-State Electron. **28**, 81 (1985), and references therein].
- ¹²S. Okuma, T. Terashima, and N. Kokubo, Solid State Commun. **106**, 529 (1998).
- ¹³S. Okuma and N. Kokubo, Phys. Rev. B **61**, 671 (2000).
- ¹⁴N.-C. Yeh, D. S. Reed, W. Jiang, U. Kriplani, C. C. Tsuei, C. C. Chi, and F. Holtzberg, Phys. Rev. Lett. **71**, 4043 (1993).
- ¹⁵For example, see Fig. 2(a) or Fig. 1(a) in Ref. 10.
- ¹⁶D. Ephron, A. Yazdani, A. Kapitulnik, and M. R. Beasley, Phys. Rev. Lett. **76**, 1529 (1996).
- ¹⁷M. V. Feigel'man, V. B. Geshkenbein, and A. I. Larkin, Physica C **167**, 177 (1990).
- ¹⁸As ρ_{ac} approaches the background level at low T (near T_g) and low f , ϕ becomes less precise. This is the reason why the low f data at low T are sometimes excluded from the f vs T plots.
- ¹⁹R. H. Koch, V. Foglietti, W. J. Gallagher, G. Koren, A. Gupta, and M. P. A. Fisher, Phys. Rev. Lett. **63**, 1511 (1989).
- ²⁰P. J. M. Wöltgens, C. Dekker, R. H. Koch, B. W. Hussey, and A. Gupta, Phys. Rev. B **52**, 4536 (1995).
- ²¹M. Charalambous, R. H. Koch, T. Masselink, T. Doany, C. Feild, and F. Holtzberg, Phys. Rev. Lett. **75**, 2578 (1995).
- ²²S. Okuma and H. Hirai, Physica B **228**, 272 (1996).
- ²³T. Nojima, A. Kakinuma, and Y. Kuwasawa, Phys. Rev. B **56**, 14 291 (1997).
- ²⁴H. K. Olsson, R. H. Koch, W. Eidelloth, and R. P. Robertazzi, Phys. Rev. Lett. **66**, 2661 (1991).
- ²⁵J. Kötzler, M. Kaufmann, G. Nakielski, R. Behr, and W. Assmus, Phys. Rev. Lett. **72**, 2081 (1994).
- ²⁶S. Okuma and N. Kokubo, Phys. Rev. B **56**, 14 138 (1997).
- ²⁷In the case of thin (2D) films, the intersection point B_{ST}^{2D} is more clearly determined, because the ($T=0$) SIT occurs at this point.
- ²⁸H. Ishida and R. Ikeda, J. Phys. Soc. Jpn. **71**, 254 (2002).
- ²⁹G. Blatter and B. Ivlev, Phys. Rev. Lett. **70**, 2621 (1993).
- ³⁰G. Blatter, B. Ivlev, Y. Kagan, M. Theunissen, Y. Volokitin, and P. Kes, Phys. Rev. B **50**, 13 013 (1994).
- ³¹T. Onogi and S. Doniach, Solid State Commun. **98**, 1 (1996).
- ³²R. Ikeda, Int. J. Mod. Phys. B **10**, 601 (1996).
- ³³A. Krämer and S. Doniach, Phys. Rev. Lett. **81**, 3523 (1998).
- ³⁴E. M. Chudnovsky, Phys. Rev. B **51**, 15 351 (1995).
- ³⁵A. Rozhkov and D. Stroud, Phys. Rev. B **54**, R12 697 (1996).
- ³⁶P. H. Kes, M. H. Theunissen, and B. Becker, Physica C **282-287**, 331 (1997).
- ³⁷J. A. Chervenak and J. M. Valles, Jr., Phys. Rev. B **61**, R9245 (2000).
- ³⁸In order to reproduce the experimental value of $\Delta B_{QVL}=0.08$ for the 300-nm-thick film with Eq. (1), we must use $c_L = 0.17$ ($\nu = 1$). This value is again of reasonable magnitude but higher than $c_L=0.12$ for the 100-nm-thick film.
- ³⁹M. P. A. Fisher, Phys. Rev. Lett. **65**, 923 (1990).
- ⁴⁰It has been reported recently [D. R. Strachan, M. C. Sullivan, P. Fournier, S. P. Pai, T. Venkatesan, and C. J. Lobb, Phys. Rev. Lett. **87**, 067007 (2001)] that the collapse of dc I - V data onto scaling functions proposed by Fisher *et al.*² alone does not prove the existence of VGT. The authors have proposed a criterion to determine if the data collapse is valid, and thus if the phase transition occurs. They have claimed that none of the data reported in the literature meet their criterion. We believe that our data of ac and dc resistivities measured simultaneously for thick In (Ref. 26) and $a\text{-Mo}_x\text{Si}_{1-x}$ (Ref. 10) films are most naturally interpreted in terms of VGT, while we must be careful in claiming the phase transition from the dc data alone.
- ⁴¹P. Berghuis, A. L. F. van der Slot, and P. H. Kes, Phys. Rev. Lett. **65**, 2583 (1990).
- ⁴²Ali Yazdani, W. R. White, M. R. Hahn, M. Gabay, M. R. Beasley, and A. Kapitulnik, Phys. Rev. Lett. **70**, 505 (1993).
- ⁴³A. Kapitulnik, A. Yazdani, J. S. Urbach, W. R. White, and M. R. Beasley, Physica B **197**, 530 (1994).
- ⁴⁴A. C. Marley, M. J. Higgins, and S. Bhattacharya, Phys. Rev. Lett. **74**, 3029 (1995).
- ⁴⁵A. M. Petrean, L. M. Paulius, W.-K. Kwok, J. A. Fendrich, and G. W. Crabtree, Phys. Rev. Lett. **84**, 5852 (2000).
- ⁴⁶G. Blatter, M. V. Feigel'man, V. B. Geshkenbein, A. I. Larkin, and V. M. Vinokur, Rev. Mod. Phys. **68**, 1125 (1994).
- ⁴⁷L. I. Glazman and A. E. Koshelev, Phys. Rev. B **43**, 2835 (1991), and references therein.
- ⁴⁸Y. Yeshurun and A. P. Malozemoff, Phys. Rev. Lett. **60**, 2202 (1988).
- ⁴⁹We have obtained the data consistent with this picture using 4-nm-thick (2D) $a\text{-Mo}_x\text{Si}_{1-x}$ films, although direct verification of the 2D VGT at $T=0$ has not yet been performed (Ref. 8).
- ⁵⁰E. S. Sadki, Z. H. Barber, S. J. Lloyd, M. G. Blamire, and A. M. Campbell, Phys. Rev. Lett. **85**, 4168 (2000).
- ⁵¹Y. Kuwasawa, K. Kato, M. Matsuo, and T. Nojima, Physica C **305**, 95 (1998).